

NEAR-WALL MEASUREMENTS OF TURBULENCE STATISTICS WITH LASER DOPPLER VELOCITY PROFILE SENSORS

Katsuaki Shirai, Christian Bayer, Andreas Voigt,
Thorsten Pfister, Lars Büttner, Jürgen Czarske

Technische Universität Dresden
Chair of Measurement and Testing Techniques
Department of Electrical Engineering and Information Technology
Helmholtzstraße 18, 01069, Dresden, Germany
Tel: +49-(0)351-463-36192
Fax: +49-(0)351-463-37716
shirai@iee.et.tu-dresden.de
<http://eeemp1.et.tu-dresden.de>

ABSTRACT

We report on the evaluation of the near-wall turbulence statistics in a fully developed channel flow. The measurement was conducted with laser Doppler velocity profile sensors. The sensor provides both the information of lateral velocity and axial position of individual tracer particles inside the measurement volume, which yields the velocity profile inside the measurement volume without being mechanically traversed. Hence, velocity measurement with a high spatial resolution up to micrometer resolution is achieved without strongly reducing the size of the measurement volume. The streamwise velocity was measured with two independent velocity profile sensor systems at three different Reynolds number conditions. The resulting turbulence statistics show a good agreement with available data of direct numerical simulations up to the fourth order moments. This demonstrates the velocity profile sensor to be one of the promising techniques for turbulent flow research with the advantage of a spatial resolution more than one order of magnitude higher than a conventional laser Doppler technique.

INTRODUCTION: BACKGROUND AND SCOPE

Discussions have been continuing on the scaling and dependency of turbulence statistics on Reynolds number in turbulent boundary layers. Many approaches have been made both with experiments and numerical simulations, and they provided precious information on the mechanisms and the structure of turbulence. However, still some open questions remain, in particular toward filling the gap between the flow in laboratory and realistic conditions. One of such is the existence of universality and scaling of turbulence statistics in a high Reynolds number flow. The difficulty of the issue originates mainly in the lack of spatial resolution of both measurement techniques and numerical simulations at high Reynolds number conditions, since the basis of the discussion stands on well-converged statistically independent set of data covering wide range of Reynolds number conditions. Continuous progress of computers and numerical simulation schemes would afford to simulate higher Reynolds number flows, which provide us more insight on the three dimensional behavior of flow structures. In experimental investigations, the existence of high shear rate as well as small scale structures in a high Reynolds number flow requires suf-

ficiently high spatial resolution to avoid the spatial averaging effect of the sensor. The existing experimental techniques are known to suffer from the spatial averaging effect when the scale of interest becomes relatively small compared to the sensing area of the sensor. Such measurements could lead to biased understandings on the measurement results.

The laser Doppler velocity profile sensor, which has been proposed to overcome the spatial averaging of conventional laser Doppler anemometry (Czarske et al. 2001, Czarske 2001, Czarske et al. 2002). The velocity profile sensor enables the determination of particle's axial position as well as transverse velocity using two non-parallel fringe systems inside the measurement volume. Since the position of particle path can be determined inside the measurement volume, the sensor has a resolution at least one magnitude of order higher than a conventional technique (typically of the order of micrometers range). The real spatial resolution in a fluid flow about a few micrometers was demonstrated in a measurement of a micro channel (Bayer et al. 2007). The first application of the velocity profile sensor to a turbulent flow was reported in Shirai et al. (2006a), in which mean and rms distributions of the streamwise velocity were shown for a single Reynolds number condition. However, the higher order moments and the statistics in different Reynolds number conditions have not been reported.

This paper reports on the near-wall turbulence statistics in a turbulent channel flow. The main purpose of the study is to investigate the possible dependency and the scaling of turbulence statistics at different Reynolds number conditions in a turbulent boundary layer. Two independent velocity profile sensor systems were built up with major improvements on optics and electronics for stable operation. The flow condition was carefully prepared for achieving the stationary two-dimensional flow. The main focus in the present measurements is paid to obtain large number of independent set of data. The effect of spatial resolution on the measured turbulence statistics will be systematically investigated by changing the spatial resolution of the measurement. Such data would give some insights on the possible Reynolds number effect and the existence of universality at high Reynolds numbers. In this paper the first phase of the measurement results are provided with the two velocity profile sensor systems. The statistics are reported up to fourth order mo-

ment with three different Reynolds number conditions, and they are compared with available direct numerical simulation (DNS) data.

VELOCITY PROFILE SENSOR

Flow measurements were carried out with a novel laser Doppler velocity profile sensor. The principle of the sensor is based on the use of two fringe systems in a single measurement volume. Since the details of the principle are described in the former papers (Czarske et al. 2001, Czarske 2001, Czarske et al. 2002), it is briefly described here. In contrast to a conventional laser Doppler technique (e.g., Durst et al. 1976, Tropea et al. 1995, Albrecht et al. 2003), the profile sensor employs two pairs of beams with non-parallel fringe systems. One of the fringe systems is diverging and the other is converging in the direction of optical axis (y axis in this paper). The measured pair of Doppler frequencies corresponding to the two fringe systems provides the position as well as velocity of individual tracer particles. Since the fringe spacing curves are unique functions of the coordinate along the optical axis, the position can be precisely known from the calibration through the quotient of the Doppler frequencies pair. From the measured position, the local fringe spacing is determined and hence the velocity is obtained according to the calibration. Because of the spatial resolution inside the measurement volume, high spatially resolved velocity measurement is achieved. The positional determination accuracy is proved to be independent of the magnitude of the velocity and the relative accuracy of the velocity measurement is higher than a conventional laser Doppler anemometry (Czarske et al. 2002).

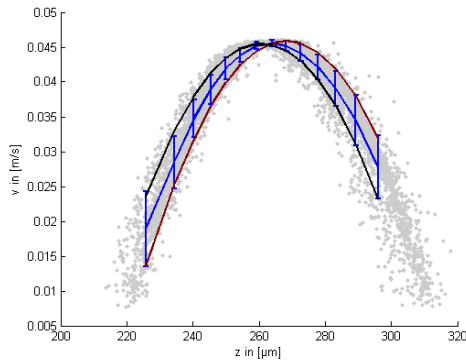


Figure 1: Velocity profile measured with a WDM sensor in a micro channel with a nominal width of $100 \mu\text{m}$. The real spatial resolution was estimated to be about $3.5 \mu\text{m}$ by shifting the parabolic fit to the raw velocity profile.

Two different sensor systems were used for the flow measurements. They were realized with two different techniques, wavelength-division multiplexing (= WDM) and frequency-division multiplexing (= FDM). The difference is the methods used for discriminating the two fringe systems (refer to the review by Czarske (2006) for details). Hereafter, they are called as WDM and FDM sensor based on the techniques, respectively. For the details of the respective method, a reader can refer to Czarske et al. (2001), Czarske (2001) and Czarske et al. (2002) for the WDM sensor and Pfister et al. (2005) and Shirai et al. (2006a) for the FDM

sensor. The WDM system discriminates the signal from two fringe systems by using two different wavelengths of light, while two different carrier frequencies are used in the FDM system for that purpose. Major improvements were made for the stable operation of the sensor systems during long time of measurement. The WDM sensor utilized two single-mode laser diodes with different wavelengths as laser sources. Dichroic mirrors were employed for combining and separating the two wavelengths. The WDM sensor was not equipped with fiber optics and with any frequency shift technique, which is in general aimed at the measurements of reverse flow and small velocity close to zero. However, the measurement of velocity close to the wall was still possible to be accomplished with a method described in Bayer et al. (2007). This was achieved by applying a dynamic filtering technique in a self-made MATLAB processing software. The real spatial resolution was also investigated in a measurement of micro-channel flow. Fig. 1 shows one of the results obtained in a two-dimensional micro-channel of $100 \mu\text{m}$ width. A parabolic velocity profile was obtained without using any averaging nor filtering of data points. The WDM sensor used for the measurement did not have to be traversed. The channel width of $101 \mu\text{m}$ calculated from the measurement result shows an excellent agreement with the nominal value of $100 \mu\text{m}$. The spatial resolution was estimated to be $3.5 \mu\text{m}$ from the standard deviation of the data scattering in the measurement (further details are described in Bayer et al. 2007). The FDM sensor utilized three acousto-optic modulators (AOMs) to generate two carrier frequencies and fiber-optics was used for the robustness and flexibility of the system. The measured signals were mixed down with the carrier frequencies and the pedestal part was removed before the signal evaluation. The laser source was upgraded to a DPSS (diode-pumped solid-state) Nd:YAG laser with the wavelength of 532 nm , the output optical power of 150 mW , the beam quality of $M^2 < 1.1$ and the rms noise level of less than 0.2% ($10 \text{ kHz} - 100 \text{ MHz}$). The available optical power was much increased in the measurement volume (factor of about five compared to the former system (Pfister et al. 2005), which advantageously improves the quality of measurement signals. The measurement head was exchanged to a newly designed one with the beams aligned in a plane for improving the signal quality. The electronics was also upgraded from Mini-Circuits components to an integrated one with some additional filters for suppressing noise in the unwanted frequency ranges. These upgrades significantly increased the signal to noise ratio compared to the former FDM systems and the number of outliers was dramatically reduced.

The effect of the insertion of a glass plate between the sensor and the measurement volume was investigated. It shifts the paths of the laser beams due to the refraction at the glass plate surfaces. Care must be taken so that the beams are crossing at a single spatial point to create the measurement volume. As long as the plate is positioned so that the glass surface is perpendicular to the optical axis of the sensor, the measurement volume is just shifted in position compared to the configuration without the glass plate being inserted (see Fig. 2). The figure shows that the calibration curve remains unchanged when the glass plate is placed at the two different positions 1 and 2. It gives an

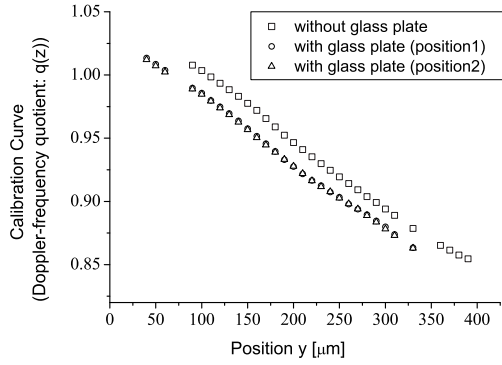


Figure 2: Effect of glass plate inserted between the measurement head and the measurement volume. The calibration curve remains unchanged as long as the measurement head is traversed perpendicular to the glass plate.

important indication that the calibration curve is not affected by traversing of the sensor. This fact ensures the validity of a single calibration curve for all the velocity measurements conducted with traversing, as long as the head is traversed perpendicular to the glass plate (i.e., wall). Furthermore, it turned out that the thickness of the glass plate does not cause a serious effect but rather the glass material and possibly surface quality affects the signal quality, hence the effective length of the measurement volume (Shirai et al. 2006b). The calibration of the sensor and the flow measurements were carefully carried out through the glass plate with the same material and thickness as used for the flow measurement.

FLOW APPARATUS AND VELOCITY PROFILE SENSOR

The flow to be measured was the turbulent boundary layer in a fully developed channel flow. The basic flow configuration was the same as reported in Zanoun et al. (2003) and Shirai et al. (2006a). Here only the essence is described for clarity. The flow medium was air at normal room temperature and DEHS (diethylhexyl sebacate) was seeded for tracer particles from the upstream of the blower inlet. The cross-sectional dimensions of the channel were 50×600 mm (aspect ratio of 1:12), which was sufficient to be considered as two-dimensional flow. The measurements were carried out at the position of 6.2 m (corresponds to $248 h$; h : channel half-width) downstream from the channel inlet, where the flow was expected to be fully developed. Along the centerline of the channel, static wall pressure taps were equipped for monitoring the pressure gradient in the streamwise direction. The fully developed condition was confirmed in the downstream of about 2.5 m from the inlet by the linear pressure gradient along the streamwise direction. In the measurement section, a pair of glass plates was attached flush to both the top and bottom walls of the channel to have optical access and not to disturb the flow (see Fig. 3). It should be emphasized that the pair of glass plates was attached in order to avoid unfavorable effect caused by sudden expansion when only a single glass plate is attached at the end of the channel (Shirai et al. 2006a). This is supposed to be the reason for the deviation of the mean velocity distribution compared to generally reported ones in the former measurement.

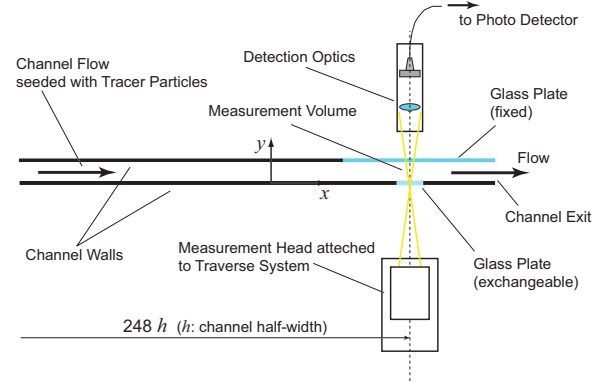


Figure 3: Flow measurement configuration in the channel flow. Two glass plates were mounted flush to the wall to have an optical access but not to disturb the flow. The sensor has a spatial resolution in side the measurement volume in the direction of optical axis.

Table 1: Characteristics of the sensors and the measurement conditions (L : working distance, l_y : length of the measurement volume in y direction, σ_y : spatial resolution, σ_U/U : relative accuracy of velocity measurement, u_τ : friction velocity, $Re_\tau (= u_\tau h/\nu)$: Reynolds number, l_τ : viscous length scale)

| sensor type | L [mm] | l_y [μm] | σ_y [μm] | σ_U/U [%] | u_τ [m/s] | Re_τ | l_τ [μm] |
|-------------|----------|------------|-----------------|------------------|----------------|-----------|---------------|
| WDM | 80 | 500 | 1.5 | 0.06 | 0.26 | 420 | 60 |
| WDM | 80 | 350 | 1.5 | 0.06 | 0.49 | 780 | 32 |
| FDM | 310 | 900 | 6 | 0.085 | 0.71 | 1100 | 23 |

RESULTS

The nominal parameters of the both sensors are shown in Table 1. For signal processing an online method based on the technique proposed in Shirai et al. (2005) was applied to determine the particle position and velocity. The original program was extended into online one with additional validation steps being implemented (Bayer et al. 2007). A correction scheme was employed using the weighting function based on the inverse of the instantaneous velocity (McLaughlin and Tiederman 1973) in order to reduce the velocity bias caused by the steep velocity gradient close to the wall. According to the report by Edwards et al. (1987) on the statistical bias problems in laser anemometry, this scheme is not recommended and residence-time weighting scheme should be used. However, residence time was not recorded in the present experiment and the scheme based on the inverse of the instantaneous velocity still did work since the measured velocity component matched the direction of the dominant mean flow as pointed out by Hoesel and Rodi (1977).

The measurements were conducted with three different Reynolds number conditions with two different sensors as listed in Table 1. The coordinates x , y , z were taken so that they corresponds to the streamwise, wall-normal, spanwise direction, respectively as shown in Fig. 3. The dimensions of the measurement volume were both approximately $100 \mu\text{m}$ in x and z direction based on the beam diameter at the crossing point. The Reynolds number is based on the friction velocity $u_\tau = \sqrt{\tau_w/\rho}$ (τ_w : wall shear stress, ρ : density) and the channel half-width h . The friction velocity was determined from the streamwise wall-static pressure gradient. The estimation accuracy of the wall shear stress and the friction velocity was estimated to be 3-4 % and 2-3 % (with

95 % confidence level), respectively. The three experimental conditions were chosen based on the following concept. The first condition ($Re_\tau=420$) was chosen in order to focus on the measurement close to the wall. Hence, the data were collected mainly in the near-wall region. The second condition ($Re_\tau=780$) was chosen to investigate the use of different glass plates as well as Reynold number compared to the first case. The third condition ($Re_\tau=1100$) was chosen to see the effect of the different sensor systems and the Reynolds number compared to the other two conditions. Relatively large amounts of data were taken in the intermediate region for this condition.

The turbulence statistics of streamwise velocity are shown in Fig. 4 up to fourth order central moment. The statistics shown in Fig. 4 are the mean and rms velocity normalized with the friction velocity, third-order (skewness factor: $\overline{u'^3}/(\sqrt{\overline{u'^2}})^3$) and fourth-order central moments (flatness factor: $\overline{u'^4}/(\sqrt{\overline{u'^2}})^4$) (u' : fluctuating velocity). The horizontal axis was normalized with the viscous length scale $l_\tau (= \nu/u_\tau)$. For comparison, available DNS data by Abe et al. (2001) at $Re_\tau = 640$ and by Iwamoto et al. (2002) at $Re_\tau=400$ and 640 are shown in the plots. The error bars in the present experiment are shown also in the plots. They were dominated by the random errors in the flow measurements and the systematic errors of the sensors shown in Table 1 were negligible compared to the statistical ones due to the finite size of samples. The error bars shown in the mean velocity indicate the measurement uncertainty with 95 % confidence level. The error bars for the higher order moments indicate the measurement uncertainty (standard deviation) calculated by the method described in Benedict and Gould (1996).

The statistics were calculated using a constant-width slot-technique. Due to the continuous distribution of the data points measured with the velocity profile sensor, the data had to be distributed into slots with finite width in order to calculate the statistics. This means that the statistics were calculated for the data within a slot with a defined width. A new outlier-reduction scheme based on the local linear fit (Shirai et al. 2006b) was applied with a cutoff threshold of four times the standard deviation in the slot and with 50 % overlap of neighboring slots. The number of points reduced by this scheme was at most 5 % out of the total data points depending on the data set. The slot width was empirically chosen for each set of the measurement data so that the statistical convergence and the spatial resolution became balanced. Different width of slots were applied for mean and higher order moments (rms, skewness, flatness) and they are listed in Table 2. In the vicinity of the wall, very few samples were collected due to the low density of the tracer particle in the near-wall region. The data sets in several slots close to the wall and the furthest slot from the wall were omitted from the statistics shown in Fig.4 since there were very few number of data points and the statistical uncertainty increased dramatically in such slots.

The mean velocity distributions are shown in Fig. 4(a). They are well scaled with wall variables and show good agreements with the DNS data. The wall shear stress was independently estimated from the near-wall data points with the method suggested by Cenedese et al. (1998) using the

Table 2: Slot width used for calculating the turbulence statistics

| Re_τ | mean | | rms, skewness, flatness | |
|-----------|---------------------------------|---------------------|---------------------------------|---------------------|
| | slot width [μm] | samples per slot | slot width [μm] | samples per slot |
| 420 | 30 | 400 | 140 | 1700 |
| 780 | 80 | 450 | 160 | 850 |
| 1100 | 50 | 650 | 120 | 1450 |

data points lying in the region $y^+ < 10$. The wall shear stress estimated from the mean velocity shows an excellent agreement within the measurement uncertainty for the lowest Reynolds number condition ($Re_\tau=420$). In the two higher Reynolds number cases ($Re_\tau=780$ and 1100), slight deviations toward higher velocity are observed for the data in the near-wall region. This is supposed to be caused by some remaining effect which could not be corrected by the velocity bias correction scheme. Relatively small numbers of data were obtained in the near wall region for these cases. It should also be taken into account that small deviation is emphasized in the logarithmic scale in the wall-normal direction in the Fig. 4(a). In the highest Reynolds number condition ($Re_\tau=1100$), the logarithmic velocity profile is apparently observed in the region apart from the wall, however, it is necessary to take more data points in order to make reliable estimation of the coefficients of the logarithmic law of the wall in the overlap region. It is noteworthy that the velocity data were obtained down to very close to the wall for the lowest Reynolds number case ($Re_\tau=420$) with the WDM sensor, with which no frequency shifting technique was equipped. The closest point obtained for this condition was at $y^+ \approx 1.2$, corresponding to the physical value of 72 μm in the height from the wall and about 0.3 m/s in velocity.

The rms distributions are shown in Fig. 4(b). They are also well scaled with the wall variables and show good agreements with the DNS data again. The maximum rms values are consistent with generally reported values. The position of the maximum is also well coincident with the position where the turbulence production has its peak in the buffer layer. The present data show some trend of the rms peak depending on the Reynolds number. This might be some possible indication of low Reynolds number effect. A higher number of data points is required to make further arguments on the Reynolds number effect. The rms statistics shows still some scatter in the overlap region. This is also an indication that a higher number of data points per slot is required to make further statements on the rms statistics with a high spatial resolution.

The third and fourth order moments (skewness and flatness factors) are shown in Fig.4(c, d). They show excellent scalings with wall variables close to the wall, and the agreement with the DNS data (Iwamoto et al. 2002) is reasonable. Further comparison of the statistics in the overlap region for different Reynolds number conditions would be possible with a higher number of data points taken in the intermediate region for the two lower Reynolds number conditions ($Re_\tau=420$ and 780). Only the data at the highest Reynolds number condition ($Re_\tau=1100$) is available in the early part of overlap region and it shows fairly good agreement with the DNS data. The statistics show scatter in the region mainly due to the relatively low number of data points used

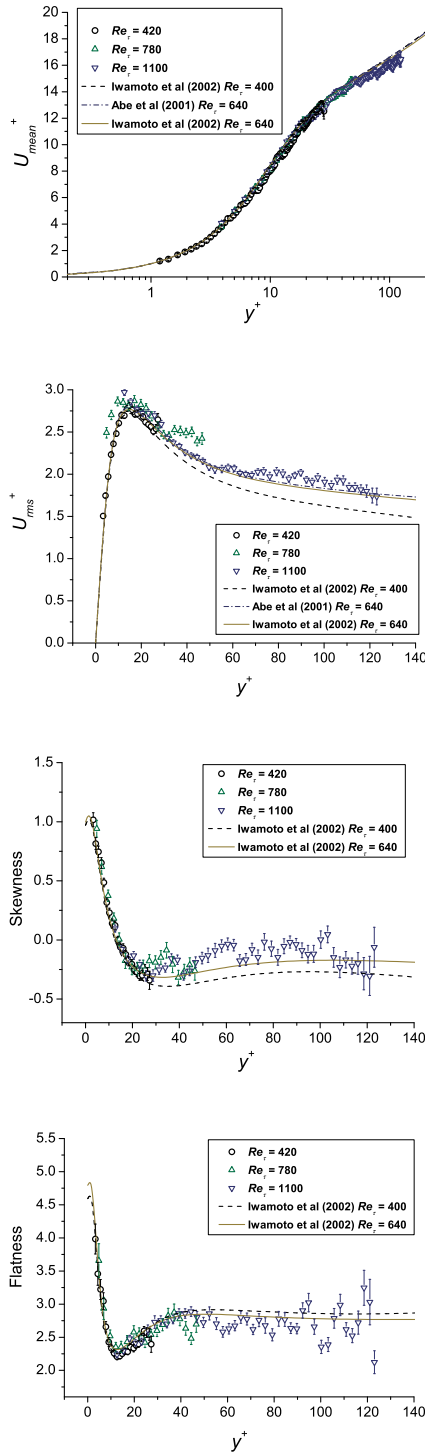


Figure 4: Turbulence statistics at three different Reynolds numbers compared with available DNS data. (a) mean velocity (left top), (b) rms velocity (right top), (c) skewness factor (left bottom), (d) flatness factor (right bottom)

for calculating the higher order moments. The measured skewness factor shows a systematic deviation compared to the DNS data. The reason for this deviation cannot be explained clearly at the moment, but it should be noticed that the DNS data by Iwamoto et al. (2002) used for the comparison was at about half the Reynolds number ($Re_\tau=400$

and 640) compared to that of the present measurement data ($Re_\tau = 1100$). In the DNS data both skewness and flatness factors have a peak close to the wall and their value decrease slightly approaching toward the wall. This behavior was not possible to be observed from the present data set and further investigation close to the wall is planned for clarifying this point.

DISCUSSION

As a consequence the velocity profile sensor was demonstrated to be a promising technique for high spatially resolved measurement of turbulence statistics in a turbulent boundary layer. The different realization of the two sensor systems did not yield any discernible difference on the measurement results. Both the sensor systems worked well in the present measurement. The only difference was the complexity of the systems and the validated data rate during the measurement. The WDM system was simple and relatively easy to adjust compared to the FDM system, which utilized complex electric circuits to operate the AOMs and required careful adjustment of optics. The valid data rate was lower for the WDM system due to the particle passing outside the measurement volume, while the rate for the FDM system was kept high through the measurement. The higher valid data rate was because the down-mixing equipped in the FDM system effectively reduced unmodulated signals from outside the measurement volume before the signal detection. It turned out that sufficient amount of data per slot should be taken for obtaining credible statistics up to higher order moments. In order to provide the turbulence statistics with a spatial resolution comparable to the estimated spatial resolution of the sensors, more number of data has to be taken in the measurement. Providing such data is indeed challenging since all the flow conditions must be well controlled to keep the flow state constant during the measurements in order to obtain credible statistics with a high spatial resolution. The authors monitored the deflection of the glass plate (i.e., wall) at the measurement location with the same condition as the flow measurements using a laser triangulation sensor (sample rate: 2.5 kHz, spatial resolution: 1 μm). It appeared that a periodic oscillation of $\pm 35 \mu\text{m}$ amplitude existed in the wall normal direction at the high Reynolds number condition ($Re_\tau = 1100$) in the present measurements (Shirai et al. 2006b). This amplitude already exceeded the estimated spatial resolution of the sensor by one order of magnitude, and hence it does not make much sense to provide statistics with a spatial resolution higher than the oscillation amplitude of the flow apparatus itself. Therefore, we would emphasize that a well controlled flow condition is crucial for such reliable measurements of turbulence statistics with a high spatial resolution as well as the high capability of a sensor. An alternative is to compensate the wall deflection by monitoring it during the measurement. With a sufficient care of flow condition, taking more data points per slot would give us more insight on the structure of the near-wall turbulence and possible Reynolds number effect for higher order moments in a high Reynolds number flow with confidence.

CONCLUDING SUMMARY

The application of a velocity profile sensor to the near-wall

regions of a fully developed turbulent channel flow was reported. The flow measurements were conducted with two different sensor systems at three different Reynolds number conditions. The turbulence statistics of the streamwise velocity up to fourth order moment was calculated with high spatial resolution. The measured mean and rms velocity distributions scaled well with the wall variables in the near-wall region and they showed good agreements with available DNS data. The third and fourth order moments were also calculated and showed relatively good agreement with available DNS data. For the higher order moments (rms, third and fourth order moments), even some possible dependence of the statistics on Reynolds number was observed. Both the sensor systems realized with different techniques worked well without giving any discernible difference on the measurement results. Taking more data samples with well controlled flow conditions would provide credible data up to higher order moments with full resolution of the sensors. Such data would also give insights on the detailed structure of turbulence near the wall and possible Reynolds number effect on higher order moments at a high Reynolds number condition. The work is ongoing toward obtaining credible statistical data in the near-wall region of a turbulent boundary layer. In conclusion, the laser Doppler velocity profile sensor has been demonstrated to be a promising technique for such an investigation of turbulent flows where a high spatial resolution is required.

ACKNOWLEDGMENTS

Dr. G. Yamanaka, Dr. S. Becker, Mr. H. Lienhart and Prof. F. Durst are acknowledged for their supports and fruitful discussions on the flow measurements in the LSTM Erlangen. Prof. D. Petrak is acknowledged for giving us opportunity to measure the micro-channel flow. The support from the Deutsche Forschungsgemeinschaft (DFG) is greatly appreciated (CZ55/20-1).

REFERENCES

H. Abe, H. Kawamura, Y. Matsuo (2001) "Direct numerical simulation of a fully developed turbulent channel flow with respect to Reynolds number dependence", *Trans. ASME J. Fluids Eng.*, Vol. 123, pp. 382-393.

H. Albrecht, M. Borys, N. Damaschke, C. Tropea (2003) "Laser Doppler and phase Doppler measurement techniques", Springer, Heidelberg.

C. Bayer, A. Voigt, K. Shirai, L. Büttner, J. Czarske (2007) "Interferometrischer Laser-Doppler-Feldsensor zur Messung der Geschwindigkeitsverteilung von komplexen Strömungen", (in German) *Technisches Messen*, Vol. 74, pp. 224-234.

L.H. Benedict, R.D. Gould (1996) "Towards better uncertainty estimates for turbulence statistics", *Exp. Fluids*, Vol. 22, pp. 129-136.

A. Cenedese, G.P. Romano, R.A. Antonia (1998) "A comment on the "linear" law of the wall for fully developed turbulent channel flow", *Exp. Fluids*, Vol. 25, pp. 165-170.

J. Czarske, L. Büttner, T. Razik, H. Welling (2001) "Measurement of velocity gradients in boundary layers by a spatially resolving laser Doppler sensor", *Proc. SPIE*, Vol. 4448, pp. 60-71.

J. Czarske (2001) "Laser Doppler velocity profile sensor using a chromatic coding", *Meas Sci Technol*, Vol. 12, pp. 52-57.

J. Czarske, L. Büttner, T. Razik, H. Müller (2002) "Boundary layer velocity measurements by a laser Doppler profile sensor with micrometre spatial resolution", *Meas. Sci. Technol*, Vol. 13, pp. 1979-1989.

J. Czarske (2006) "Laser Doppler velocimetry using powerful solid-state light sources", *Meas. Sci. Technol.*, Vol. 17, pp. R71-R91.

F. Durst, A. Melling, I. H. Whitelaw (1976) "Principles and Practice of Laser-Doppler Anemometry", Acad. Press, New York

R.V. Edwards (ed.) (1987) "Report on the special panel on statistical particle bias problems in laser anemometry", *Trans. ASME J. Fluids Eng.*, Vol. 109, pp. 89-93.

W. Hoesel, W. Rodi (1977) "New biasing elimination method for laser-Doppler velocimeter counter processing", *Rev. Sci. Instrum.*, Vol. 48, pp. 910-919.

K. Iwamoto, Y. Suzuki, N. Kasagi (2002) "Reynolds number effect on wall turbulence: toward effective feedback control", *Int. J. Heat and Fluid Flow*, Vol. 23, pp. 678-689.

J.C. Klewicki, R.E. Falco (1990) "On accuracy measuring statistics associated with small-scale structure in turbulent boundary layers using hot-wire probes", *J. Fluid Mech.*, Vol. 219, pp. 119-142.

D.K. McLaughlin, W.G. Tiederman (1973) "Biasing correction for individual realization of laser anemometer measurements in turbulent flows", *Phys. Fluids*, Vol. 16, pp. 2082-2088.

T. Pfister, L. Büttner, K. Shirai, J. Czarske (2005) "Monochromatic heterodyne fiber-optic profile sensor for spatially resolved velocity measurements with frequency division multiplexing", *Appl. Opt.*, Vol. 44, pp. 2501-2510.

K. Shirai, T. Pfister, J. Czarske (2005) "Signal processing technique for boundary-layer measurements with a laser-Doppler velocity-profile-sensor", *Proceedings of the GALA-Fachtagung 13: Lasermethoden in der Strömungsmesstechnik*, 6-8th September 2005, Cottbus, Germany, pp. 4.1-4.8.

K. Shirai, T. Pfister, L. Büttner, J. Czarske, H. Müller, S. Becker, H. Lienhart, F. Durst (2006a) "Highly spatially resolved velocity measurements of a turbulent channel flow by a fiber-optic heterodyne laser-Doppler velocity-profile sensor", *Exp. Fluids*, Vol. 40, pp. 473-481.

K. Shirai, C. Bayer, T. Pfister, L. Büttner, J. Czarske, H. Müller, G. Yamanaka, H. Lienhart, S. Becker, F. Durst (2006b) "Measurement of universal velocity profile in a turbulent channel flow with a fiber-optic profile sensor", *Proceedings of the 13th Int. Symp. on Applications of Laser Techniques to Fluid Mechanics*, Lisbon, Portugal, 26-29th June 2006, Paper 1.3.1-12.

C. Tropea (1995) "Laser Doppler anemometry: recent developments and future challenges", *Meas. Sci. Technol.*, Vol. 6, pp. 605-619.

E.-S. Zanoun, F. Durst, H. Nagib (2003) "Evaluating the law of the wall in two-dimensional fully developed turbulent channel flows", *Phys. Fluids*, Vol. 15, pp. 3079-3089.